Preparation and characterization of a novel composite microporous polymer electrolyte for Li-ion batteries

CHEN Zuofeng[1], JIANG Yanxia[1],
ZHUANG Quanchao[1], DONG Quanfeng[1, 2],
WANG Ye[1] & SUN Shigang[1]

1. State Key Laboratory for Physical Chemistry of Solid Surfaces, Department of Chemistry, Xiamen University, Xiamen 361005, China;
2. Powerlong Battery Research Institute, Xiamen University, Xiamen 361005, China

Correspondence should be addressed to Jiang Yanxia or Sun Shigang (email: yxjiang@xmu.edu.cn or sgsun@xmu.edu.cn)

Abstract **A novel composite microporous polymer electrolyte composed of poly(vinylidene fluoride-co-hexafluoropropylene) (PVdF-HFP) and mesoporous SBA-15 was prepared. The composite solid polymer electrolyte (CSPE) exhibits ionic conductivity as high as 0.30 mS·cm^{-1} with a composition of SBA-15：PVdF-HFP=3：8 at room temperature. Infrared transmission spectroscopic results suggested that the mechanism of micropore formation is similar to that of the phase inversion. X-ray diffraction (XRD) results demonstrated that the addition of SBA-15 inhibits the crystallization of PVdF-HFP, while the SBA-15 preserves well its ordered mesoporous structure during the course of preparation. The Li/CSPE/MCF of half-cell was assembled, and it showed a good electrochemical and cyclability performance during charge-discharge cycles.**

Keywords: lithium ion batteries, microporous polymer electrolyte, PVdF-HFP, mesoporous SBA-15.

Polymer lithium ion batteries (PLIB), commonly referred to as the second generation lithium ion batteries, have received much attention since the first introduction by Bellcore Corp.[1, 2]. The concept suggested by Bellcore Corp. to construct a PLIB is based on the preparation of a microporous polymer, and the immobilization of liquid electrolyte in the microporous polymer matrix. Nowadays, the separator in the Bellcore system is prepared with extraction step, i.e. it is first to prepare PVdF-HFP/plasticizer (such as dibutyl phthalate (DBP)) blend film, and then remove the plasticizer by liquid extraction using a low boiling point solvent, leaving the porous matrix in the film. However, the extraction step will complicate the industrial production process. Moreover, since the boiling point of plasticizer is usually comparatively high, it is not

easy to remove all the residual plasticizer by drying, thus resulting in a poor cyclability performance of the cell. Phase inversion[3, 4] is another method in common use to prepare the microporous film. In this type of approach, double solvents with different volatility and dissolvability for PVdF-HFP are used to form phase separation in the drying course of the mixed solution. In comparison with the Bellcroe's technique, phase inversion can be done avoiding a complex extraction step, yet the method requests strict conditions of temperature and humidity to control the solvent evaporation. It tends to fail on a little poor controlled condition, thus, the application of phase inversion is not practical in industrial production. In order to improve the method further, substantial research efforts have been devoted[5, 6], and other methods are introduced to prepare PVdF-HFP microporous film. For example, Wang et al.[5] developed a new easy method to prepare microporous film without extraction step with the blend of PVdF-HFP and poly(vinyl pyrrolidone) (PVP).

SBA-15 is a new type of mesoporous molecular sieve or silica that was synthesized firstly by Zhao in 1998 [7]. This material possesses a highly ordered hexagonal arrangement of cylindrical mesopores that accounts for the easy entrance and transfer in comparison with the microporous materials such as zeolite. In addition, noticing that the SiO_2 is widely used as inorganic filler in polymer electrolyte, SBA-15 consists of SiO_2 with the tetrahedron framework unit, and exhibits steady electrochemical properties. Because of their numerous merits, applications of SBA-15 in rechargeable lithium or lithium ion batteries have attracted attention by degrees in recent years. Reddy et al.[8] explored modification of a polyethylene oxide (PEO) with mesoporous SBA-15, and the conduction mechanism was studied in the composite system. Jiang and coworkers[1] also developed a composite PEO with LiAlSBA, and the ionic conductivity examined at 30℃ was enhanced with 3 or 4 orders of the magnitude. In this work, SBA-15 composite microporous polymer electrolytes were prepared based on a new type of craftwork, in which no plasticizer was applied and it does not need to involve the extraction step. Moreover, comparing with phase inversion, the requirement for the temperature and humidity was undemanding in the course of preparation.

1 Experimental

1.1 Materials

A copolymer of PVdF-HFP, trade mark Kynar Flex 2801, was provided by Elf Atochem. Mesoporous SBA-15 was used as filler to make the microporous film, and NaY

1) Li, X. L., Zhao, Y., Jiang, Z. Y. et al., The 12th National Conference on Electrochemistry (in Chinese), 2003.

ARTICLES

zeolite was used for comparison. An electrolyte solution with 1 mol/L $LiPF_6$ in EC / DMC / EMC (volume ratio 1∶1∶1) was provided by Mitsubishi Chemical. All other chemicals were of analytical grade.

1.2 Membrane preparation

A certain amount of SBA-15 powder was dispersed in the DMF solvent by ultrasonic, and then the quantitative PVdF-HFP polymer of 0.40 g was dissolved in the above mixture, and stirred to facilitate dissolution. After complete dissolution, the mixture was cast on a newly cleaned glass plate with a fixed area and desired thickness was made with the approach of self-spread. The solvent was evaporated in a dry atmosphere to form a film (about 80 μm), designated as the dry film. The dry film thus obtained was activated by adding liquid electrolyte to it in a glove box after further drying under vacuum, designated as the wet film. In comparison with the Bellcore's technique, the approach of preparing microporous membranes in this paper is denominated as the direct-making-pore technique (DMPT).

1.3 Characterization and instruments

Porosity was measured by the following method: Immerge the dry film into *n*-butanol for 2 h, weigh the mass of membrane before and after absorption of *n*-butanol, then calculate the porosity of membrane based on the following equation: $P\% = (W_w - W_d)/(\rho_b \cdot V_p)$, where W_w and W_d are the mass of the wet film and dry film, respectively, ρ_b is the density of *n*-butanol, and V_p the volume of the dry film. The electrolyte uptake, R_A was defined as the ratio of the mass of absorbed electrolyte solution (m_s) to the mass of the dry film (m_p), i.e. $R_A = m_s/m_p$. The ionic conductivities of the composite film were determined by complex impedance spectra on CHI660 B electrochemical workstation (Chenhua Corp., Shanghai China). The wet film was sealed between two stainless steel electrodes. The measurements were performed in the frequency range from 100 kHz to 10 Hz. The bulk resistance of the polymer electrolyte was found from impedance spectrum, where the intercept on the real axis gave the value. The conductivity was calculated based on the following equation: $\sigma = L/(R \cdot S)$, where σ is the conductivity, R the bulk resistance, L the thickness of the specimen, S the area of the specimen.

The surface morphology of the composite electrolyte was observed by using scanning electron microscope (SEM, LEO 1530) with gold sputtered-coated films. Fourier Transform Infrared (FTIR) transmission spectroscopic measurements were carried out on a Nexus 870 FTIR spectrometer (Nicolet) equipped with an EverGlo IR source and a liquid nitrogen-cooled MCT-A detector. A home-made IR transmission cell was employed with two

CaF_2 disks used as the IR windows, and the samples were sealed between the two CaF_2 disks in a sandwiched manner. In the transmission FTIR experiments, the single-beam spectrum of background (R_B) was collected at first, and then the transmission single-beam spectra of samples (R_{Si}) were collected. The resulting spectrum was expressed as conventional absorption spectrum, i.e. $A = -\log(R_{Si}/R_B)$. X-ray diffraction (XRD) patterns, recorded in small and big angle respectively, were done on X' pert PRO diffractometer with K_α of Cu target as radiant point, as well as tube voltage of 40 kV and tube current of 30 mA.

The charge and discharge tests were carried out on Xinwei electrochemical workstation at a constant current density and within the voltage range of 1.5−0.002 V. The anode used was lithium metal. The cathode active material was mesophase-pitch-based carbon filer (MCF), furthermore, carbon black and PVdF-HFP were used as conductivity aid and binder, respectively. The cathode slurry comprising the above material was cast on a treated copper current collector with N-methylpyrrolidone (NMP) as solvent. The activated composite solid polymer electrolyte (SBA-15∶PVdF-HFP = 3∶8 in weight ratio) was used as separator and electrolyte between the cathode and the anode to form a coin cell, nominated as Li/CSPE/MCF.

2 Results and discussion

2.1 Morphology of the SBA-15 composite film

SEM image of the SBA-15 composite film is shown in Fig. 1. It can be seen that the membrane shows uniform network-like micropore structure. The average pore diameter of the sample is determined to be less than 10 μm. By contrast, the NaY composite polymer membrane prepared under the same condition displays compact structure without any pores. The different types of molecule sieve exhibit remarkable influence on the morphology of mem-
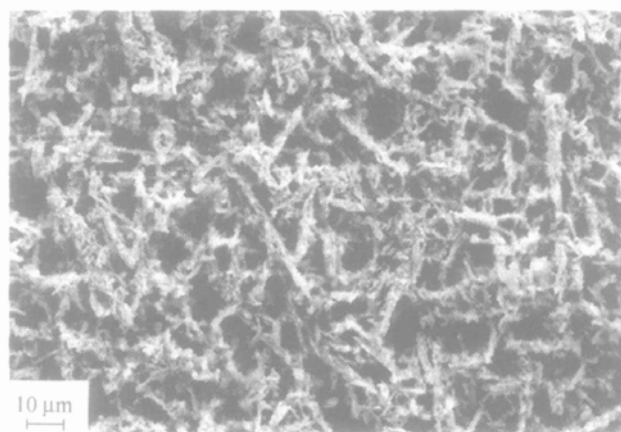

Fig. 1. SEM image of SBA-15 composite polymer electrolyte membrane, SBA-15; PVdF-HP=3∶8 in weight ratio.

Table 1 Comparison of porosity, electrolyte uptake and conductivity of composite polymer electrolyte

	SBA-15/g					NaY/g	SBA-15/g (Bellcore's technique[1,2])
	0.20	0.15	0.10	0.05	0.00	0.15	0.15
Porosity	51.4%	35.8%	14.8%	6.5%	3.3%	6.7%	44.4%
Electrolyte uptake	76.0%	50.2%	28.5%	17.7%	11.8%	38.5%	95.8%
Conductivity/mS·cm^{-1}	0.63	0.30	0.025	0.009	0.0053	0.013	1.42

brane. For comparison, the blend membrane using SBA-15 as common filler was prepared by Bellcroe's technique[1,2], which presents loose sponge-like micropore structure. The difference in the morphologies is directly related to the mechanism of micropore formation.

2.2 Studies of the porosity, electrolyte uptake and ionic conductivity

The experimental data of porosity, electrolyte uptake and ionic conductivity of the samples are listed in Table 1. It can be seen that the porosity, electrolyte uptake and ionic conductivity were enhanced rapidly with the increase of SBA-15 mass. In the case of the composite film containing 0.15 g SBA-15, the ionic conductivity is as high as 0.3 mS·cm^{-1} at room temperature, which is about two orders of magnitude higher than that of the blank film. The temperature dependence of the ionic conductivity, i.e. the plot of $\log \sigma$ versus 1/T, is approximately linear, suggesting Arrhenius-like behavior of ionic conduction in a limited temperature range (25℃—80℃). With the further increase of the mass of SBA-15, though the ionic conductivity keeps improving, the mechanical strength falls to a certain extent. It is worthwhile to note that the composite membrane is affected slightly by the glass substrate, resulting in a skin layer in the bottom surface, which inhibits the increase of the ionic conductivity. By contrast, the NaY composite film with compact structure shows a limited conductivity improvement, which is only 2 times larger than that of the blank film. Besides, for the SBA-15 composite film based on Bellcroe's technique[1,2], it exhibits largest conductivity of 1.4 mS·cm^{-1}, attributed to the less skin layer in the membrane.

2.3 IR studies of mechanism of micropores formation

In order to figure out the mechanism of the micropores formation, FTIR transmission spectroscopic studies were carried out. Fig. 2(a) shows the IR absorption peaks of the mesoporous SBA-15 owing to the presence of the oxygen-hydrogen single bond (O-H) at 3420 cm^{-1} and 1628 cm^{-1}, as well as of the silicon-oxygen single bond (Si-O) at 1092 cm^{-1}, which is consistent with those reported in ref. [9]. Fig. 2(b) displays the IR spectrum of DMF solvent, in which the adsorption peak ascribed to C=O double bonds appears around 1657—1696 cm^{-1}[10]. The IR spectrum of SBA-15 containing a little DMF solvent is presented in Fig. 2(c). It can be seen that the O-H IR band

of 1628 cm^{-1} shifts positively to 1658 cm^{-1} and becomes broader. In addition, a slight positive-shift of this band is also observed in the range of C=O adsorption. This may be attributed to the interaction between the Si−OH in SBA-15 and nitrogen atom in DMF solvent. The schematic representation in Fig. 3 suggests the interaction of hydrogen bond between SBA-15 and DMF. Fig. 2(d) and (e) illustrates IR spectra of PVdF-HFP blank film and SBA-15 composite PVdF-HFP film after drying in air for 12 h at 70℃, respectively. The IR band of Si-OH in SBA-15 and C=O in solvent DMF are observed respectively around 1655 and 1708 cm^{-1} in Fig. 2(e). The peak position of O-H band in Fig. 2(e) is the same as that in Fig. 2(c), which may suggest that the interaction between SBA-15 and PVdF-HFP is likely weak. On the other hand, it may indicate the existence of strong interaction between DMF and Si-OH, since it is not easy to remove DMF from the composite film in the presence of SBA-15. Such interaction will induce the conglomeration of DMF within and outside the SBA-15 mesochannel, then bring on the
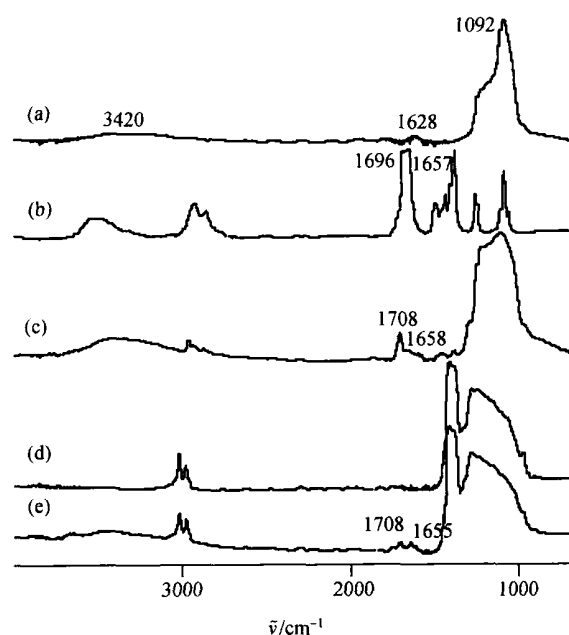
Fig. 2. The IR spectra of (a) SBA-15; (b) DMF; (c) SBA-15 containing a little DMF; (d) PVdF-HFP blank film; (e) SBA-15 composite PVdF-HFP film.

SBA-15 solvate, finally engender a new type of solvent phase around SBA-15.

Based on the above results and discussions, it is reasonable to presume that there may exist two states of solvent in the mixture of DMF, PVdF-HFP and SBA-15, i.e. simple solvent state of DMF (DMF$_{sol}$) and the state of solvent adsorbed around SBA-15 (DMF$_{SBA-15}$). The former possesses a low boiling point and exhibits strong solvency for PVdF-HFP, whereas the latter reversed. In comparison with the phase inversion in a common sense, the mechanism of micropores formation in the SBA-15 composite can be suggested as follows: The mixture thus confected is cast on a newly cleaned glass plate. Since the boiling point of DMF$_{SBA-15}$ is much higher than that of DMF$_{sol}$, the mass of DMF$_{SBA-15}$ and PVdF-HFP may keep invariable while the DMF$_{sol}$ is vaporizing. Following the evaporation of DMF$_{sol}$, the system of the confected mixture comes into the mesophase region, then initiates further a disassembling phenomenon, sequentially forming the rich and deficient phase of PVdF-HFP. The polymer in the rich phase crystallizes to form the microporous framework gradually, simultaneously the deficient phase turns into pores infilling the polymer film. At the end of the phase inversion, PVdF-HFP and SBA-15 in the deficient phase attach to the matrix, producing the SBA-15 crystallite covered with PVdF-HFP.
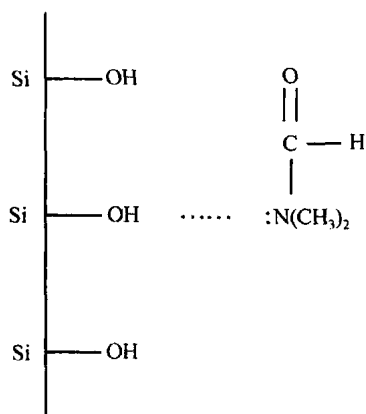

Fig. 3. Schematic representation for the interaction between SBA-15 and DMF solvent.

2.4 XRD characterization of the SBA-15 composite polymer electrolyte

Fig. 4 presents the small angle XRD patterns of SBA-15 powder, PVdF-HFP blank film and the SBA-15 composite PVdF-HFP film. It can be seen from Fig. 4(a) that the SBA-15 powder exhibits the structure of typical hexangular phase at 2θ in the range of $0.5°-2°$, attributed to the characteristic diffraction peaks of (100), (110) and (200), respectively[7]. For the PVdF-HFP blank film

shown in Fig. 4(b), the XRD pattern does not exhibit any diffraction peaks. The curve in Fig. 4(c) is enlarged 15-fold for comparison. We can still observe the characteristics of the three crystal planes in SBA-15, indicating that the ordered mesochannel arrangement of SBA-15 has not been destroyed in the preparation process. Besides, the reduction in intensity may be due to the existence of PVdF-HFP inside and outside the SBA-15 channel. The integrality of the ordered structure in SBA-15 takes on basilic significance for the formation of micropores of the composite polymer electrolyte and the cyclability performance of Li-ion batteries.
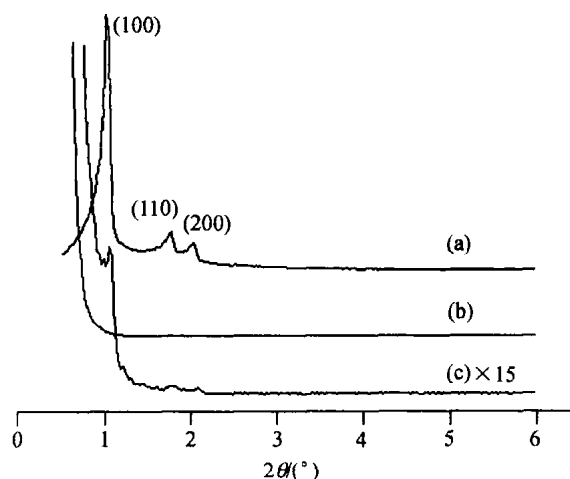

Fig. 4. Small angle XRD patterns of (a) SBA-15; (b) PVdF-HFP blank film; (c) SBA-15 composite PVdF-HFP film.

Fig. 5 displays the patterns concerning the crystallinity change of samples by the big angle X-ray diffraction. The characteristic diffraction peaks of semi-crystalline PVdF-HFP powder appear between $2\theta=15°$ and $2\theta=40°$, and comprise two sharp diffraction peaks at $2\theta=17.8°$ and $19.5°$, as well as two wide diffraction peaks at $2\theta=26.2°$ and $38°$, which can be associated with the (100)+(020), (110), (021) and (002) reflections of crystalline PVdF, respectively[11-13]. The XRD pattern of PVdF-HFP blank film is shown in Fig. 5(b), in which the diffraction peak at $2\theta=38.0°$ disappears and the other diffraction peaks become less prominent, indicating the decrease of crystallization degree in PVdF-HFP blank film. With the addition of the mesoporous material to PVdF-HFP polymer electrolyte, the intensity of peaks decreases further, attended with diffraction peak at $2\theta=26.2°$ disappearing and diffraction peak at $2\theta=17.8°$ converging into one hump, as shown in Fig. 5(c). The results suggest that the PVdF-HFP crystallinity is further reduced by the mesoporous SBA-15. It can be considered that the presence of SBA-15 blocked and separated the continuous

crystallinity growth at the end of the phase inversion. The deterioration of PVdF- HFP crystallinity will improve the electrolyte uptake and the self-plasticity, leading to an enhanced conductivity.

2.5 Cyclability of lithium ion batteries

In order to verify the electrochemical performance of the composite polymer electrolytes, coin cells of Li/CSPE /MCF were assembled to test their performance of charge-discharge cycling. A typical charge-discharge curve of the first cycle at a constant current density of 0.1 C between 1.5 and 0.002 V is shown in Fig. 6. The charge-discharge plateau is stable, and the coulombic efficiency of the first

Fig. 7. Long-term cycling tests of the Li/CSPE/MCF cell at a constant current density of 0.5 C.

cycle is around 85.0% attributed to the formation of SEI film. The relative values of charge capacities as a function of cycle numbers from 2 to 20 are shown in Fig. 7. The charge capacity decreases slightly and remains 94.0% of the initial capacity after 20 cycles, which proves a good cyclability performance of Li/CSPE/ MCF cell with an SBA-15 composite polymer electrolyte.

3 Conclusion

Composite microporous polymer electrolyte based on the blend of SBA-15 and PVdF-HFP was prepared. Conductivity of the composite film was found to be as high as 0.30 mS·cm^{-1} at room temperature when SBA-15 : PVdF-HFP=3 : 8. The temperature dependence of the ionic conductivity exhibits Arrhenius-like behavior. Studies of infrared transmission spectroscopy illustrated the interaction between Si-OH in SBA-15 and nitrogen atom in DMF solvent, which led to the formation of micropores. The XRD results indicated that the addition of SBA-15 inhibits the crystallization of PVdF-HFP to a certain extent, while the SBA-15 preserves the mesoporous structure well during the course of preparation. The battery of Li/CSPE/ MCF using the composite microporous polymer electrolyte was assembled. The coulombic efficiency of the first cycle is around 85.0% and the cell remains 94.0% of the initial capacity after 20 cycles, demonstrating the potential application of the composite polymer electrolyte in the lithium ion batteries.
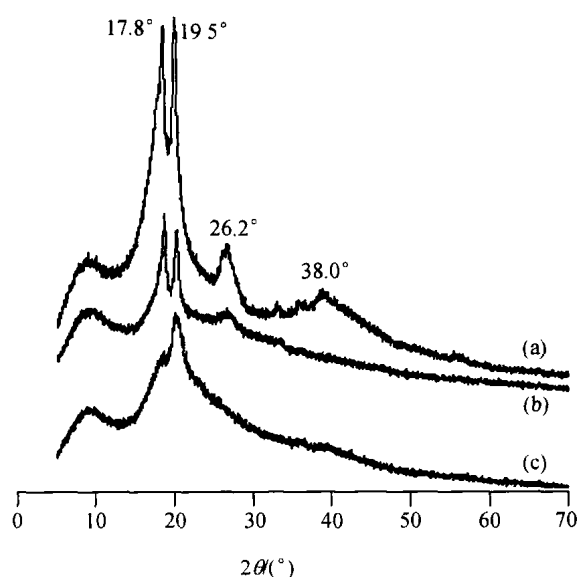

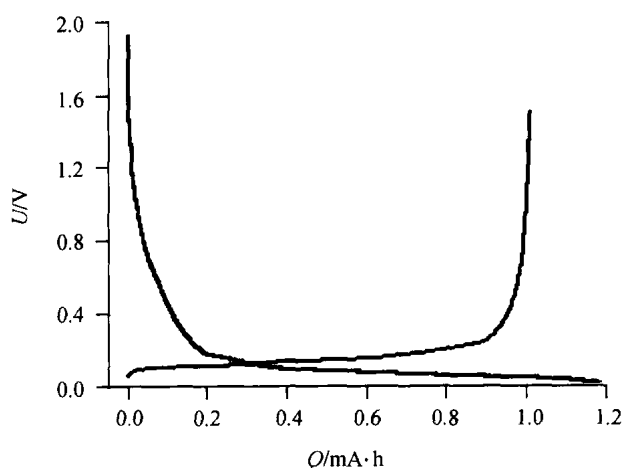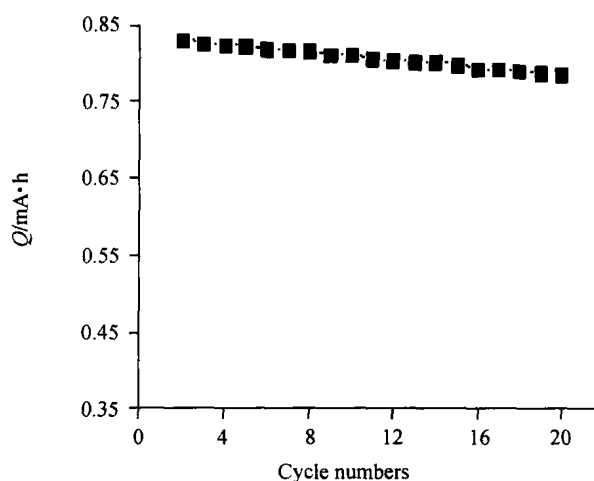Fig. 5. Big angle XRD patterns of (a) PVdF-HFP powder; (b) PVdF-HFP blank film; (c) SBA-15 composite PVdF-HFP film.

Fig. 6. Charge-discharge curve of the first cycle of the Li/CSPE/MCF cell at a constant current density of 0.1 C.

ARTICLES

References

1. Gozdz, A. S., Scumutz, C. N., Tarascon, J. M., Rechargeable lithium intercalation battery with hybrid polymeric electrolyte, US Pat., 5 296 318, 1993-03-06.

2. Tarascon, J. M., Goztz, A. S., Schmutz, C. et al., Performance of Bellcore's plastic rechargeable Li-ion batteries, Solid State Ionics, 1996, 86-88: 49−54.

3. Arcella,V., Sanguineti, A., Quartarone, E. et al., Vinylidenefluoride-hexafluoropropylene copolymers as hybrid electrolyte components for lithium batteries, J. Power Sources, 1999, 81-82: 790−794.

4. Boudin, F., Andrieu, X., Jehoulet, C. et al., Microporous PVdF gel for lithium-ion batteries, J. Power Sources, 1999, 81-82: 804−807.

5. Wang, Z. L., Tang, Z. Y., Characterization of the polymer electrolyte based on the blend of poly (vinylidene fluoride-co-hexa-fluoropropylene) and poly (vinyl pyrrolidone) for lithium ion battery, Materials Chemistry and Physics, 2003, 82: 16−20.

6. Kim, D. W., Sun, Y. K., Electrochemical characterization of gel polymer electrolytes prepared with porous membranes, J. Power Sources, 2001, 102: 41−45.

7. Zhao, D. Y., Feng, J. L., Huo, Q. H. et al., Triblock copolymer syntheses of mesoporous silica with periodic 50 to 300 angstrom pores, Science, 1998, 279(23): 548−552.

8. Jaipal Reddy, M., Chu, P. P., ^{7}Li NMR spectroscopy and ion conduction mechanism in mesoporous silica (SBA-15) composite poly(ethylene oxide) electrolyte, J. Power Sources, 2004, 135: 1−8.

9. Guo, C., Zhang, D., Jin, G. X., Mesoporous zeolite SBA-15 supported nickel diimine catalysts for ethylene polymerization, Chinese Science Bulletin, 2004, 49(3): 249−253.

10. Wang, Z. X., Huang, B. Y., Lu, Z. H. et al., Vibrational spectroscopic studies of interactions between $LiClO_4$ and the plasticizer dimethylformamide, Solid State Ionics, 1996, 92: 265−271.

11. Saikia, D., Kumar, A., Ionic conduction in P(VDF-HFP)/PVDF–(PC + DEC)–$LiClO_4$ polymer gel electrolytes, Electrochimica Acta, 2004, 49(16): 2581−2589.

12. Abbrent, S., Plestil, J., Hlavata, D. et al., Crystallinity and morphology of PVdF–HFP-based gel electrolytes, Polymer, 2001, 42: 1407−1416.

13. Tawansi, A., Oraby, A. H., Abdelkader, H. I. et al., $FeCl_3$-$CoCl_2$ mixed fillers effects on the structural, electrical and magnetic properties of PVDF films, J. Magnetism and Magnetic Materials, 2003, 262: 203−211.

The catalytic behavior of La-Mn-O nanoparticle perovskite-type oxide catalysts for the combustion of the soot particle from the diesel engine

WANG Hong[1,2], ZHAO Zhen[1], XU Chunming[1], LIU Jian[1] & LU Zhixiao[2]

1. State Key Laboratory of Heavy Oil Processing, University of Petroleum, Beijing 102249, China;
2. Beijing Institute of Petrochemical Technology, Beijing 102617, China
Correspondence should be addressed to Zhao Zhen (email: zhenzhao@ bjpeu.edu.cn)

Abstract The $La_{1-x}M_x MnO_3$(M=Li, Na, K, Rb, x=0, 0.10, 0.25) perovskite-type oxides whose sizes are nanoparticle have been prepared by the citric acid-ligated method. The characters of the catalysts were characterized by means of XRD, IR, SEM and BET surface area measurement. The catalytic activity for the combustion of soot particulate was evaluated by a technique of the temperature-programmed reaction. In the $LaMnO_3$ catalyst, the partial substitution of alkali metal (Li, Na, K, Rb) into A-site enhanced the catalytic activity for the combustion of soot particle. The $La_{0.75}K_{0.25}MnO_3$ oxides are good candidate catalysts for the soot particle removal reaction, and the combustion temperatures of soot particle are between 285℃ and 430℃ when the contact of catalysts and soot is loose, and their catalytic activities for the combustion of soot particle are as good as supported Pt catalysts, which is the best catalyst system so far reported for soot combustion under loose contact conditions.

Keywords: perovskite-type oxides, diesel exhaust, carbon particulate, alkali metals, catalyst.

The main contaminations emitting from diesel engines contain soot particulate, carbon monoxide, nitrogen oxide, hydrocarbon and so on. Soot particulate, whose surface was covered with organic contamination, heavy metal and many other matters arousing cancerization, is the main factor bringing about odour and visible aerosol in the auto pollution, and it is necessary to control and restrict soot contamination emitting from diesel engines.

The most promising technology in the field of soot removal is based on wall-flow type catalytic traps, periodically regenerated by the combustion of soot. The temperature of diesel exhaust gases, generally between 150℃ and 450℃, is lower, however, the combustion of the trapped soot is at above 550℃[1]. The role of the catalyst here is to reduce soot combustion temperature and en-